The accuracy of criteria for automatic 3-D graphics reconstruction of bone from computer tomography

THE ACCURACY OF CRITERIA FOR AUTOMATIC 3-D GRAPHICS RECONSTRUCTION OF BONE FROM COMPUTER TOMOGRAPHY

P. Rothuizen*, L. van Erning** and R. Huiskes*

Lab. Experimental Orthopaedics* and Department of Diagnostic Radiology**, University of Nijmegen, Nijmegen, The Netherlands

1. INTRODUCTION

The purpose of this study was to develop an automatic contour detection procedure to reconstruct the three-dimensional geometry of bones with Computer Tomography for automatic mesh generation in finite element analysis and for purposes of artificial joint design.

The application of Computer Tomography, for the quantification of bone geometry, bone density and morphology of bony structures is meeting increasing popularity in Orthopaedic Biomechanics (1-5). The method is attractive not only as a result of its nondestructive nature, but also because the information obtained is directly available in numerical form as a cross-sectional matrix of relative X-ray attenuation coefficients or CT-values. Hence, this data is directly applicable in principle for automatic 3-D graphics computer reconstructions.

The first objective is to determine the inner and outer contours of the cortex per cross-section. In a CT-image these contours are visualized rather than quantified; due to limitations in resolution they do not appear as distinct discontinuities in the CT-values. Hence, to estimate their actual positions, some sort of contour criterion is needed.

Usually a specific scanner dependent window in the CT-values is set and the visible bone contours are digitized (1,5). In other cases a scanner dependent CT-value is combined with an automatic contour detection algorithm (3).

A common problem in contour detection in a proximal femoral scan is caused by non homogeneous density distributions over the cortical wall (Fig.1.). In this case a specific CT-value as contour criterion can lead to the construction of a non-closed contour. It is obvious that the actual cortical contours do not coincide with any specific CT-value in this case.

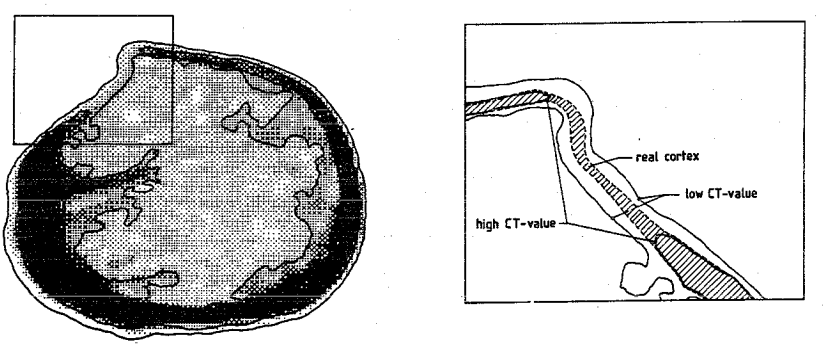

FIGURE 1 : Typical example of density distributions in a proximal femoral cross-section in a Computer Tomography image matrix.

As a result of these effects it is difficult to accurately reconstruct the bone geometry without any kind of visual interference of the operator. To overcome this problem and to make accurate automatic contour detection possible, an algorithm based on a relative contour detection procedure was developed, using individual X-ray attenuation profiles.

The subject of this paper is the contour detection procedure and its accuracy. To investigate the accuracy two comparative studies were done, one using bone phantoms with known dimensions and one using a proximal femur.

All objects were scanned in a Siemens Somatom DR3 CAT-scanner using a slice thickness of 2 mm, an image matrix of 512 * 512 pixels and a 520 mAs product at a tube voltage of 125 kV.

2. THE AUTOMATIC CONTOUR DETECTION PROCEDURE

The automatic contour detection procedure developed can be subdivided in three successive stages:

1. Construction of a base contour.
2. Construction of X-ray attenuation profiles.
3. Evaluation of the individual profiles.

In the first step a base contour is constructed, in such a way that the bone is with absolute certainty within the area it encloses. As a criterion for this base contour a specific CT-value is chosen. This CT-value must be higher than the CT-values of the surrounding material but lower than the CT-values of cortical bone. Detection of this base contour is performed by a search and contour following algorithm based on the evaluation of the eight neighboring pixels of each sequential matrix pixel. The contour found in this way is tested for appropriateness by calculating its length L and enclosed area A. If $L < 30\pi$, $L > 70\pi$ or $L^2/A > 10\pi$, the contour is rejected and the base CT-value is adapted until a satisfactory contour is obtained.

In the second step, lines are constructed which intersect the actual outer and inner cortical contours. In diaphyseal cross-sections, points of the base contour are connected with its geometrical center. In metaphyseal contours, proximal of the trochanter minor, lines are constructed perpendicular to this base contour. In this way profile lines are

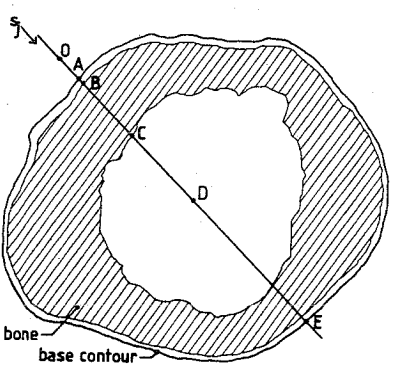

FIGURE 2.a: Profile line over a cortical wall.

constructed at intervals of approximately 1 mm, with a maximum of 1.5 mm (Fig.2.a). On each line, the attenuation profile is constructed from the attenuation matrix (Fig.2.b).

In the third step the attenuation profiles on each individual line are evaluated to estimate the unknown contour points. For this purpose two criteria were used (Fig.2.b,c). One is an absolute CT-value, C, and the other a relative CT-value, c, respectively, to estimate the actual absolute CT-value, C_b, and the actual relative CT-value, c_b, of the unknown actual contour points.

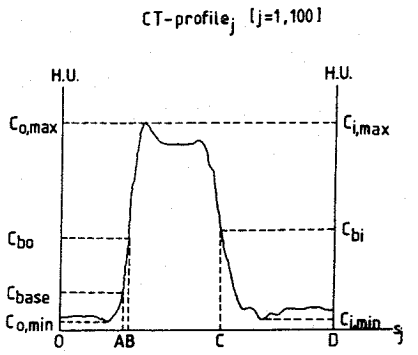

Absolute: $C = \varepsilon\,(C_{bi,j})$

Relative: $c = \varepsilon\left(\frac{C_{bi,j} - C_{i,min}}{C_{i,max} - C_{i,min}} \times 100\%\right)$

FIGURE 2.b: Typical individual relative X-ray attenuation profile in a diaphyseal cross-section of the proximal femur.

FIGURE 2.c: Criteria used to estimate actual cortical contour point positions.

The relative criteria are percentages of the total attenuation distances between the maximum and the minimum values on the periosteal and endosteal sides, respectively.

In the case that an absolute value is used, the corresponding coordinate is the estimate of the contour point. If the absolute value is higher than the maximum value on the profile, the estimated contour point defaults to the coordinate of this maximum.

When the estimates of the contour points on each profile are detected, outer and inner cortical contours are reconstructed by linear interpolation.

3. PHANTOM STUDY

The purpose of this study was twofold. First to investigate the influences of varying cortical wall thicknesses, second to evaluate the influence of trabecular bone density variations, on the accuracy and consistency of the criteria values.

Materials used were three PVC tubes with wall thicknesses 2, 5 and 9 mm. The 2 mm tube was subsequently filled with four different concentrations of calciumchloride solutions, 0, 5, 10 and 15%. All phantoms were scanned in an air environment. In each case the average tube diameter was calculated from the contour estimates, for variable absolute and relative contour criteria values C and c. Figure 3.a shows the resulting tube diameters, as functions of wall thickness, when the profiles were evaluated with the criteria C = 600 H.U. and c = 45% (which is approximately optimal for the 9 mm tube), and with c = 60%.

The graphs show that the relative criterion is more sensitive than the

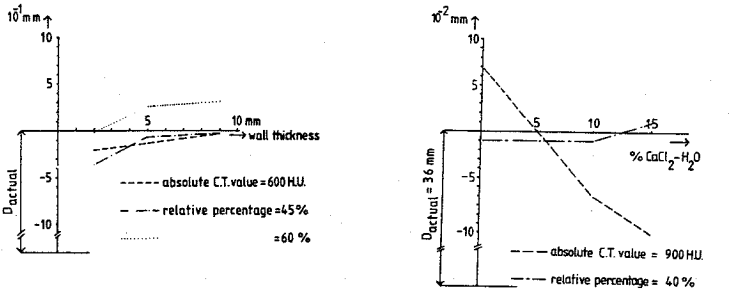

FIGURE 3.a: Accuracy of criteria chosen with varying wall thicknesses.
3.b: Accuracy of criteria chosen with varying concentrations $CaCl_2$-H_2O variations.

absolute criterion for small wall thicknesses, underestimating the actual contour diameter with 0.4 mm in the case of the 2 mm phantom. This inaccuracy, however, can be corrected for by using a relative criterion with c = 60%.

In Figure 3.b the effect of varying $CaCl_2$ concentrations on the accuracy is illustrated by showing the resulting diameter deviations from the actual diameter, using C = 900 H.U. and c = 40% as contour criteria. The absolute criterion can lead to errors in the contour diameter of up to 0.1 mm; the errors resulting from the use of the relative criterion are much smaller.

4. BONE STUDY

A proximal femur was fixed in a reference cage and scanned in polyesther, water and air environments. After scanning, the femur was sectioned at the corresponding locations. The sections were digitized and the inner and outer cortical contours compared to those obtained by the automatic contour detection procedure.

For every section separately, optimal values for the absolute and relative criteria were determined, both for the inner and the outer contours, whereby the digitized sections were considered as the true representations.

Two questions are now addressed; first, what are the optimal absolute (C, H.U.) and relative (c, %) criteria values, depending on the location in and the environment of the bone. And second, what would be the errors in contour detections if specific, consistent absolute or relative criteria values would be used in all cases.

In Figure 4 the results of the femur scanned in polyesther are summarized, in Figure 4.a relative to diaphyseal cross-sections and in Figure 4.b relative to metaphyseal cross-sections.

In the upper pair of graphs the means and variations of the optimal criteria values found are shown, for inner and outer contours, respectively; on the left for the absolute criterion (C) and on the right for the relative criterion (c).

For the diaphyseal contours it is evident that the absolute criterion

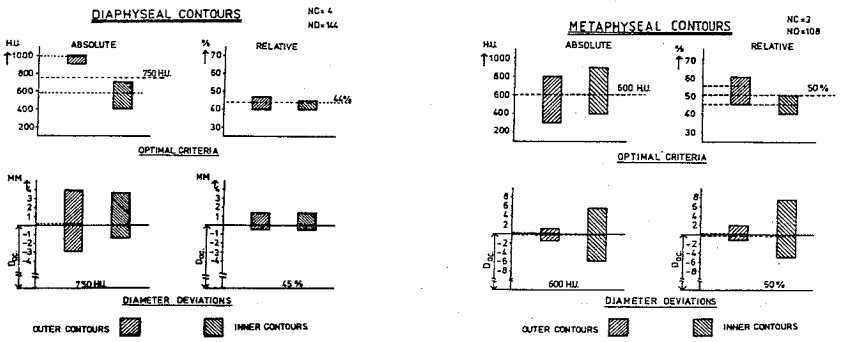

FIGURE 4.a: Optimal criteria and diameter deviations in diaphyseal cross-sections.
4.b: Optimal criteria and diameter deviations in metaphyseal cross-sections.

has different optimal values for the inner and the outer contours. Conversely, the relative optimal criterion is much more consistent and has the same value for the inner and outer contours. For the metaphyseal contours both criteria are less consistent in their optimal values, and differ slightly for the outer and inner contours.

The lower pair of graphs show the means and variations in the deviations from the true bone diameter, in the case that specific average criteria values are used. In the diaphysis C = 750 H.U. and c = 45%, and in the metaphysis C = 600 H.U. and c = 50%. Using absolute criteria, the outer diameter deviates up to 3.9 mm in the diaphysis and up to 1.6 mm in the metaphysis, the inner diameter deviates up to 3.6 mm in the diaphysis and up to 5.8 mm in the metaphysis.

Using the relative criterion, the outer diameter deviates up to 1.4 mm in the diaphysis and up to 2.0 mm in the metaphysis. The inner diameter deviates up to 1.4 mm in the diaphysis and up to 7.5 mm in the metaphysis. It must be appreciated that these are not standard deviations, but represent the maximal deviations obtained, which are sometimes exceptionally high due to the automatic character of the contour-detection procedure. In visual inspection, these peak deviations would easily be recognized and corrected.

The bone environment affects the accuracy markedly if an absolute criterion is used. Using the absolute criterion value for the femur in water to detect cortical contours of the femur in air leads to an underestimate of the mean outer cortical diameter of 0.7 mm. Using the optimal relative criterion value for the femur in water to detect cortical contours of the femur in air leads to an underestimate of the mean outer cortical diameter of 0.2 mm.

5. DISCUSSION AND CONCLUSIONS

The automatic contour detection procedure worked adequately in all cases, without any interference of the operator. Closed estimates of actual cortical contours could be processed automatically to reconstruct 3-D geometry of the proximal femur in a finite element mesh and graphically displayed as a solid model (Fig.5).

FIGURE 5 : Reconstructed 3-D geometry of the proximal femur.

Comparing the relative with the absolute criteria, it can be concluded that the relative criterion gives adequate accuracy of diaphyseal contour detection and outer cortical contour detection in the metaphysis. The absolute criterion leads to unacceptable errors in the diaphyseal region, when consistent absolute CT-values were used for both the inner and the outer cortical contours.

In the metaphyseal region of the proximal femur the results for the inner cortical contour are somewhat disappointing for both criteria, although a closed estimate of the contour was obtained in all cases.

The accuracy of the absolute criterion was markedly affected by bone environment, region of scanning and the type of contour to be detected (inner- or outer cortex).

Hence, the absolute criterion can not be set universally at a specific value. Conversily, the relative criterion can be set universally at 45%, in the diaphyseal region of the femur and at 50% to detect outer metaphyseal cortical contours, at least when using the High Resolution reconstruction algorithm on our Siemens scanner.

ACKNOWLEDGEMENT:

This study was partly sponsored by Orthopaedic Technology BV, The Netherlands.

REFERENCES

1. Garg A, Deland J, Walker PS: Design of intramedullary femoral stems using computer graphics. Eng. in Med. 2(1985)89-93.
2. McBroom RJ, Hayes WC, Edwards WT, Goldberg RP, and White AA: Prediction of vertebral body compressive fracture using quantitative computer tomography. J. Bone Jt. Surg. 67-A(1985)1206-1214.
3. Nelson PC, Robertson DD, Walker PS, Granholm JW: A computerized femoral intramedullary implant design package utilizing computer tomography data. Proceedings CAR '85, Berlin, Springer Verlag. pp.419-420, 1985.
4. Rhodes ML, Azzawi YM, Chu ES, Pang AT, Glenn WV, and Rothmann SLG: A network solution for structure models and custom prostheses manufacturing from CT data. Proceedings CAR '85, Berlin, Springer Verlag, pp.403-407, 1985.
5. Schneider E, Weber P, Gasser B, Cordey J, Robotti G, and Perren SM: Determination of geometrical and mechanical properties of the distal femur using Computer Tomography. Biomechanics X, Proceedings ISB, Sweden (in press), 1985.

COMPARISON OF OPTOELECTRONIC AND FILM BASED KINEMATIC DATA IN DYNAMIC BIOMECHANICAL EVALUATION OF BACK MUSCLE TENSION

T. Leskinen*, R. Hedberg**, B. Jonsson** and I. Kuorinka*

Institute of Occupational Health*, Helsinki, Finland and National Board of Occupational Safety and Health**, Umea, Sweden

1. INTRODUCTION

Spinal stress and its major contributor, back muscle tension, can be evaluated with biomechanical models based on the analysis of forces and torques acting on the musculoskeletal system of the human body. Postural effects due to gravity can be described by static biomechanical models (e.g. 2, 8). However, static models do not take account of the inertial forces and torques induced by acceleration, which have been found to increase the peak load on the spine by 30-60 % as compared to statically calculated loads in moderate speed lifting tasks (6, 3) and by 19 % when weights were handled on table level (7). These findings suggest that static models are of limited value when studying dynamic activities.

To analyse spinal stress biomechanically kinematic data of body postures and movements is needed. This data can be recorded on film (photography and cinematography), with video technique, and with optoelectronic methods. In principle all these methods are applicable for both two- and three-dimensional analysis, the latter facilitated by the use of two simultaneous recordings from different directions.

The dynamic analysis of spinal stress has been based on kinematic data obtained photographically using strobed light with 20 Hz (3), cinematographically with a high speed (80 frames/s) film camera (7), or optoelectronically with 100 samples/s (5). Attempts to estimate the dynamic components mathematically based on the total time of movement and photographs of the initial and final postures have also been made (1).

The film methods are time consuming especially for dynamic biomechanical purposes because they involve tedious plotting of posture from several landmarks in numerous pictures. Moreover, the manual digitizing phase causes measurement errors, which may be very serious when differentiating the raw data to obtain acceleration. However, the basic apparatus needed is cheap as compared to the other methods.

Standard video equipment have low vertical resolution and low sampling speed for dynamic analysis, but high speed high resolution equipment are available, which also facilitate automatic analysis of the data by a computer.

Optoelectronic systems allow computerized movement analysis. They all use landmarks on the body surface, which causes some sources of error: the optical connection between the landmarks and the recording apparatus (camera) must always be preserved, the cables of active (irradiating) markers may impede normal movement, passive (reflective) markers may be difficult to identify or they are rather heavy thus increasing problems arising from the movement of the landmarks on the skin.

In the dynamic biomechanical analysis the precision of the accelerations calculated is essential for the accuracy of the results. Noise in a direct movement record decreases the precision of accelerations. An increasing

signal bandwidth and a decreasing sampling frequency are factors that decrease the precision, i.e. to obtain reliable results the sampling frequency must be high enough for a specified signal bandwidth and noise level. Optimization methods have been developed for smoothing the kinematic data to minimize the noise of the calculated acceleration data (4, 9), but their use is limited to cases in which the original sampling rate is high enough.

In this study both static and dynamic biomechanical sagittal plane models were used to assess the tension of back muscles during lifts. The postures and movements of the body were recorded opto-electronically and with an 8 mm film camera. Our aim was to study if the cheap and portable but laborious film system is accurate enough for dynamic analysis of lifting.

2. MATERIALS AND METHODS

Five subjects lifted a box with handles weighing 12 kg from the initial position, the handles 25 cm from the floor, to knuckle height. The lifts were done first without instructions concerning the lifting technique (free style), and then with straight legs (back lift) and with flexed knees (leg lift). Each lift followed by lowering was repeated three times in succession.

The handles of the box were equipped with strain gauge transducers to measure the vertical force.

The movements of the body were recorded simultaneously with an opto-electronic system (Selspot) sampled 158 times/s and a Super-8 film camera with 24 frames/s. The infra-red light emitting landmarks of Selspot were attached on the knuckle of middle finger, on the elbow, on the shoulder, on the hip, on the knee, on the ankle, and on the head just in front of the ear. The elbow, ankle and head landmarks were not utilized in the biomechanical analysis. The landmarks of Selspot served as landmarks for the film analysis, too. The optoelectronic data were directly transferred to a computer disk, while the positions of the landmarks on the film had first to be digitized.

With the optoelectronic system two cameras and three-dimensional transformation were used. This system served in inhibiting parallax errors due to different distances of markers from the cameras, since only the sagittal plane coordinates were used in the analysis. A Super-8 film camera was used for the cinematographic recording. The camera was placed 4 m from the subject. A ruler with 1 m scale was placed at the same distance with the subject for length reference. The camera was equipped with electric pulse unit which gave a pulse for each frame which was exposed during the collection of the optoelectronic data. These pulses were recorded on magnetic tape together with the force signal to serve as time reference.

The same anthropometric data and biomechanical algorithms, slightly modified from those of Leskinen et al (5), were used with both types of movement data for evaluating static and dynamic components of back muscle tension. However, the optoelectronic data was first smoothed by averaging eight successive samples. The averaging window was moved so that the final sampling rate was 24 samples/s.

The muscle force estimates obtained from the two movement data were compared to each other statistically using regression analysis. Moreover, the differences of the peak forces obtained with the two methods were tested with the t-test for paired observations.

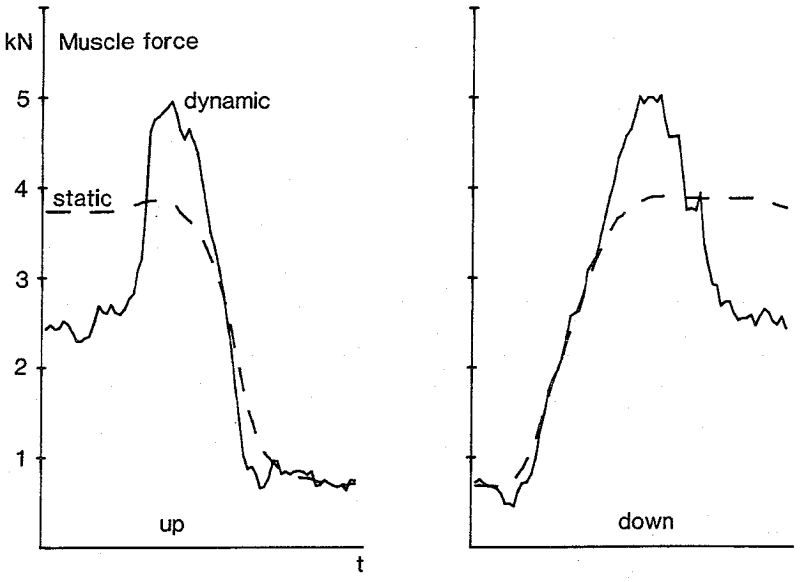

Figure 1. Static and dynamic muscle force calculated from the opto-electronic kinematic data, leg lift and lowering of subject 1.

3. RESULTS

A typical time course of dynamic and static muscle forces during lifts is presented in Fig. 1. showing that the static force is highest in the beginning of the lift, while the dynamic force reaches its peak about 100-200 ms after the start of the movement.

The linear regression of the peak forces obtained by the two methods was calculated separately for each lift and lowering. The median coefficients of correlation of static forces were 0.99 in lifting and 0.97 in lowering and those of the dynamic forces 0.83 and 0.95, respectively.

To compare the peak forces statistically, the second lift and lowering of each subject and each technique was taken for the statistical analysis. The results are presented in table 1. The static forces were systematically lower with the film method than with the optoelectronic method. A similar systematic difference was found with the dynamic peak forces in lowering, though the differences were higher than with the static forces. In lifting the differences between the dynamic forces of the two methods were often very high, and also the direction of the differences varied so that no systematic trends could be detected.

The peak vertical acceleration of the hand calculated from the opto-electronic data was in the average 2.3 ms^{-2}, and significantly lower ($p<0.01$) in lowering: 1.4 ms^{-2}. There were no statistically significant differences between the lifting techniques.

Table 1. Static and dynamic peak forces of back muscles of five subjects computed from optoelectronic (Selspot) and cinematographic (S-8) kinematic data in lifting and lowering with different techniques (the second of three successive lifts). Significance of differences: NS no significance, * $p<0.05$, ** $p<0.01$, *** $p<0.001$.

	Static force (N)			Dynamic force (N)		
	Selspot	S-8	Diff.	Selspot	S-8	Diff.
Free style						
Lifting						
mean	3552	3249	302	4706	4477	228
sd	182	297	220	417	658	444
min	3376	2860	121	4070	3793	-214
max	3850	3659	671	5243	5230	959
signif.			*			NS
Lowering						
mean	3565	3293	272	4587	3555	1032
sd	174	254	149	395	304	175
min	3373	2953	141	4212	3167	852
max	3790	3643	446	5166	3889	1277
signif.			*			***
Back lift						
Lifting						
mean	3893	3637	255	4997	5422	-425
sd	143	125	162	341	1285	1194
min	3706	3445	89	4677	3705	-1948
max	4102	3762	473	5110	6635	972
signif.			*			NS
Lowering						
mean	4020	3707	313	5091	3961	1130
sd	225	178	135	373	437	158
min	3823	3474	122	4690	3554	888
max	4409	3916	493	5549	4529	1308
signif.			**			***
Leg lift						
Lifting						
mean	3286	2887	398	4179	3698	480
sd	245	360	165	688	587	1032
min	3034	2379	205	3381	3232	-1282
max	3592	3293	655	5214	4663	1387
signif.			***			NS
Lowering						
mean	3284	2843	441	3989	3027	963
sd	295	540	252	578	604	151
min	2904	2111	174	3253	2212	699
max	3640	3405	793	4649	3578	1071
signif.			**			***

4. DISCUSSION

The static forces obtained from the film based kinematic data were systematically lower than those obtained from the optoelectronic data. However, the standard deviation of the difference was quite low suggesting that the film method gives as reliable results as the optoelectronic method in static calculations. The systematic differences mean that the scaling of distances has been different in the two methods, the film method giving smaller distances than the optoelectronic. This may arise from several factors including small errors in the calibration process of both methods, linearity errors of the cameras, and systematic errors in digitizing the films. Random errors in digitizing have no large impact in static analysis. The digitizing errors were affected by the fact that the visibility of the landmarks of Selspot was probably too poor for film digitizing purposes.

In the dynamic analysis of lowering the box the systematic difference between the results of the two methods was larger than in static calculations, because the difference in scaling of distances also makes the accelerations of the film method smaller than the accelerations of the optoelectronic method. The variation of the differences still remained in a low level. But in the dynamic analysis of lifting the differences between the methods varied very strongly to both directions suggesting that the two methods work differently from each other.

In lifting the acceleration peaks were sharper and higher and thus the frequency range of the signal was higher than in lowering. An increase in the frequency range of the signal increases the amplitude of the noise in calculated accelerations considerably, according to Lanshammar (4) with the power 2.5. Based on his work (4), a noise with the standard deviation of 1 mm in position measurements would lead to the standard deviation in acceleration of at least 0.28 ms^{-2} if the frequency range of the signal is up to 5 Hz and the sampling rate is 24 Hz, figures quite reasonable for the film analysis of lowering. If the frequency range is increased to 10 Hz (reasonable for lifting) the standard deviation of acceleration would be at least 1.6 ms^{-2}. The corresponding standard deviations for 158 Hz sampling rate would be 0.11 ms^{-2} and 0.63 ms^{-2}, respectively. These examples seem to indicate that the random errors in digitizing the films are too large for reliable calculation of accelerations in lifts with the frame rate used. A higher film speed would allow smoothing of the input data which would improve the accuracy, but it would increase the digitizing time considerably, too.

In conclusion, the film method can be used reliably for static force evaluations and even for dynamic analysis of slow movements. Although laborious, the film analysis is in many cases the method of choice being cheap and easy to use in field conditions. However, dynamic analysis of fast movements must be based on data that has been collected with a sufficiently high sampling rate. If films with normal frame rate are the only method available, they can be used to evaluate the static components of forces even in fast movements, and results of dynamic laboratory experiments (e.g. 6) may then be used for evaluating the effects of the dynamic components.

ACKNOWLEDGMENTS

This study was supported by the Finnish and Swedish Work Environment Funds.

REFERENCES

1. Ayoub, M. M. & El-Bassoussi, M. M., 1978: Dynamic biomechanical model for sagittal plane lifting activities. In Safety in manual materials handling (ed. by C. G. Drury), DHEW (NIOSH) Publication No. 78-185. U.S. Government Printing Office, Washington D.C., 88-95.
2. Chaffin, D. B., 1969: A computerized biomechanical model - development of and use in studying gross body actions. J. Biomechanics, 2, 429-441.
3. Freivalds, A., Chaffin, D. B., Garg, A. & Lee, K. S., 1984: A dynamic biomechanical evaluation of lifting maximum acceptable loads. J. Biomechanics, 17: 4, 251-262.
4. Lanshammar, H., 1982: On Precision limits for derivatives numerically calculated from noisy data. J. Biomechanics, 15: 6, 459-470.
5. Leskinen, T. P. J., Stålhammar, H. R., Kuorinka, I. A. A. & Troup, J. D. G., 1983a: A dynamic biomechanical model for the evaluation of spinal stress when lifting. Ergonomics, 26: 6, 595-604.
6. Leskinen, T. P. J., Stålhammar, H. R., Kuorinka, I. A. A. & Troup, J. D. G., 1983b: The effect of inertial factors on spinal stress when lifting. Eng Med, 12: 2, 87-89.
7. McGill, S. M. & Norman, R. W., 1985: Dynamically and statically determined low back moments during lifting. J. Biomechanics, 18: 12, 877-885.
8. Schultz, A. B. & Andersson, G. B. J., 1981: Analysis of loads on the lumbar spine. Spine, 6: 1, 76-82.
9. Woltring, H. J., 1985: On optimal smoothing and derivative estimation from noisy displacement data in Biomechanics. Human Movement Science, 4, 229-245.